journal

J. Am. Ceram. Soc., **80** [7] 1773–80 (1997)

Computer Simulation of Grain Growth and Ostwald Ripening in Alumina–Zirconia Two-Phase Composites

Danan Fan*,† and Long-Qing Chen*

Department of Materials Science and Engineering, The Pennsylvania State University, University Park, Pennsylvania 16802

The kinetics of grain growth and Ostwald ripening in Al_2O_3–ZrO_2 two-phase composites was systematically investigated using two-dimensional (2-D) computer simulations, based on a diffuse-interface field model. Using average values for the experimentally measured ratios of the grain boundary energies to the interphase boundary energy as the input, the predicted 2-D microstructural features and their evolution are in excellent qualitative agreement with experimental observations on 2-D cross sections of 3-D Al_2O_3–ZrO_2 two-phase composite microstructures. It was found that the coupled grain growth in Al_2O_3–ZrO_2 composites is controlled by long-range diffusion and the average size (R_t) as a function of time (t) follows the power-growth law, $R_t^m - R_0^m = kt$ with $m = 3$, which is independent of the initial microstructures and volume fractions of the two phases. The predicted variation of the kinetic coefficient (k) on the volume fraction follows a trend similar to that experimentally measured through the entire range of volume fractions. The scaling of grain size distributions is observed at a given volume fraction, i.e., they are time-invariant in the steady state. However, the characteristics of size distributions vary with the initial microstructures and the volume fractions. The relationship between matrix grain size and second-phase grain size is discussed.

I. Introduction

CONTROLLING grain growth and hence the grain size is a critical issue for the processing and application of advanced ceramics. One of the effective methods of controlling grain growth is by developing multiphase composites or duplex microstructures, an important example being Al_2O_3–ZrO_2 two-phase composite which, due to its toughening and superplastic behaviors, has been extensively studied.[1–6]

A schematic two-phase polycrystalline microstructure is shown in Fig. 1, in which there are three types of interfaces: grain boundaries in α (α/α) with energy $\sigma_{\alpha\alpha}$; grain boundaries in β (β/β) with energy $\sigma_{\beta\beta}$; and interphase boundaries between α and β (α/β) with energy $\sigma_{\alpha\beta}$. Coarsening of such a two-phase microstructure is driven by the reduction in the total grain and interphase boundary energy. It involves two quite different, but simultaneous processes: grain growth through grain boundary migration and Ostwald ripening via long-range diffusion. For example, in order for an α/β1 interphase boundary to move (Fig. 1), the atoms in the β1 have to dissolve into the matrix (α grains) and diffuse either through the α/α grain boundaries connected to β1 or through the matrix if there are limited mutual solubilities between α and β phases, and then reprecipitate into relatively larger β phase particles (β2–β4). The diffusion distance involved is on the order of the typical distance between β phase particles. On the other hand, in order for the grain boundary between α1 and α2 to move, atoms are required to jump from one side of the boundary to another; the diffusion distance is on the order of grain boundary width in the α phase. In a two-phase solid, the motions of a grain boundary and an interphase boundary are mutually constrained or inherently coupled. For example, the grain boundary between α1 and α2 cannot substantially move until the β1 particle entirely disappears. It may intuitively be expected that the slower process, Ostwald ripening, which involves long-range diffusion, should control the kinetics of coarsening in a two-phase solid.

There have been a few theoretical attempts to study the effect of second-phase particles on grain growth kinetics. Most of the theoretical models[7–9] made significant assumptions and Q-states Potts model simulations[10,11] considered small and immobile second-phase particles which cannot coarsen. Recently, the thermodynamics of a two-phase microstructure, in which the volume fractions of the two constituent phases are not conserved, has been analyzed by Cahn,[12] and the corresponding kinetics of grain growth and microstructural evolution were studied by Holm *et al.*[13] using the Potts model. However, the kinetics of grain growth have not been extensively investigated for two-phase systems in which the volume fractions are conserved. An important difference between a conserved system and a nonconserved one is the fact that, in nonconserved systems, long-range diffusion is not involved.

Recently, the authors have developed a diffuse-interface computer simulation model[14,15] for studying the microstructural evolution in two-phase polycrystalline materials. One of the main advantages of this model is that the complexity of microstructural evolution and long-range diffusion in two-phase materials can be automatically taken into account. Computer simulations using this model allow one not only to monitor the detailed temporal microstructure evolution during grain growth and Ostwald ripening but also to obtain all of the information about the average grain size and size distribution of all the phases.

The major purpose of this paper is to systematically study the kinetics of coupled grain growth and grain size distributions in Al_2O_3–ZrO_2 two-phase composites by employing computer simulations. For both single-phase grain growth and Ostwald ripening of second-phase particles coherently embedded in a matrix, there is strong evidence that there is a long-time scaling regime in which the shape of the grain or particle size distribution does not change with time, but the average grain size scales with time as t^n, where n is called the growth exponent. It has been generally agreed that for grain growth in a pure single phase, the growth exponent is 2,[16,17] and for Ostwald ripening of second-phase particles in a binary system, it is 3.[18]

R. Raj—contributing editor

Manuscript No. 191569. Received September 3, 1996; approved January 14, 1997.
*Member, American Ceramic Society.
Presented in part at the 98th Annual Meeting of the American Ceramic Society, Indianapolis, IN, April 15, 1996 (Basic Science Division, Paper No. SX-1-96).
Based in part on the thesis submitted by D. Fan for the Ph.D. in ceramic science and engineering, Pennsylvania State University, University Park, PA, 1996.
Supported by the National Science Foundation under Grant Nos. DMR 93-11898 and DMR 96-33719. The computing time was provided by the Pittsburgh Supercomputing Center under Grant No. DMR 940015P.
†Current address: Los Alamos National Lab, T-11, MS B262, Los Alamos, New Mexico 87545.

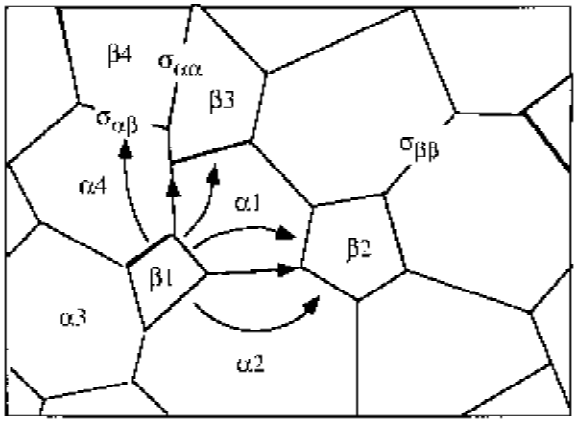

Fig. 1. A schematic two-phase microstructure.

In this paper, we will address the fundamental question whether the microstructures scale for simultaneous grain growth and Ostwald ripening in a two-phase solid. Based on the computer simulation results, we will determine the grain growth exponent. In addition, the factors which affect the grain growth and grain size distributions will be discussed. Some microstructural features predicted by the computer simulation have been previously discussed.[14,15] The details of the topological evolution and distributions in this system and other model systems is discussed in another publication.[19]

II. Diffuse-Interface Field Model

The details about this model have been reported in previous papers[14,15] and hence only a brief account of the model will be given. To describe an arbitrary two-phase polycrystalline microstructure, we define a set of continuous field variables[14,15]

$$\eta_1^\alpha(r), \eta_2^\alpha(r), ..., \eta_p^\alpha(r), \eta_1^\beta(r), \eta_2^\beta(r), ..., \eta_q^\beta(r), C(r) \qquad (1)$$

where η_i^α ($i = 1, \ldots, p$) and η_j^β ($j = 1, \ldots, q$) are called orientation field variables with each orientation field representing grains of a given crystallographic orientation of a given phase (denoted as α or β). Those variables change continuously in space and assume continuous values ranging from −1.0 to 1.0. $C(r)$ is the composition field which takes the value of C_α within an α grain and C_β within a β grain.

The total free energy of a two-phase polycrystal system, F, is then written as

$$F = \int \left[f_0(C(r);\eta_1^\alpha(r),\eta_2^\alpha(r),...,\eta_p^\alpha(r);\eta_1^\beta(r),\eta_2^\beta(r),...,\eta_q^\beta(r)) + \frac{\kappa_C}{2}(\nabla C(r))^2 + \sum_{i=1}^{p}\frac{\kappa_i^\alpha}{2}(\nabla\eta_i^\alpha(r))^2 + \sum_{i=1}^{q}\frac{\kappa_i^\beta}{2}(\nabla\eta_i^\beta(r))^2 \right] d^3r \qquad (2)$$

where ∇C, $\nabla\eta_i^\alpha$, and $\nabla\eta_j^\beta$ are gradients of concentration and orientation fields, κ_C, κ_i^α, and κ_i^β are the corresponding gradient energy coefficients, and f_0 is the local free energy density which is, in this work, assumed to be[14]

$$f_0 = f(C) + \sum_{i=1}^{p} f(C,\eta_j^\alpha) + \sum_{i=1}^{q} f(C,\eta_j^\beta) + \sum_{k=\alpha}^{\beta}\sum_{i=1}^{p}\sum_{j=1}^{q} f(\eta_i^k,\eta_j^k) \qquad (3)$$

in which

$$f(C) = -(A/2)(C - C_m)^2 + (B/4)(C - C_m)^4 + (D_\alpha/4)(C - C_\alpha)^4 + (D_\beta/4)(C - C_\beta)^4$$

$$f(C,\eta_j^\alpha) = -(\gamma_\alpha/2)(C - C_\beta)^2(\eta_i^\alpha)^2 + (\delta_\alpha/4)(\eta_i^\alpha)^4$$

$$f(C,\eta_j^\beta) = -(\gamma_\beta/2)(C - C_\alpha)^2(\eta_i^\beta)^2 + (\delta_\beta/4)(\eta_i^\beta)^4$$

$$f(\eta_i^k,\eta_j^k) = (\varepsilon_{ij}^{kk}/2)(\eta_i^k)^2(\eta_j^k)^2$$

where C_α and C_β are the equilibrium compositions of α and β phases, and $C_m = (C_\alpha + C_\beta)/2$, A, B, D_α, D_β, γ_α, γ_β, δ_α, δ_β, and ε_{ij}^{kk} are phenomenological parameters. The justification of using such a free energy model in the study of coarsening was previously discussed.[14]

The temporal evolution of the field variables is described by the time-dependent Ginzburg-Landau (TDGL)[20] and Cahn–Hilliard[21] equations,

$$\frac{d\eta_i^\alpha(r,t)}{dt} = -L_i^\alpha \frac{\delta F}{\delta\eta_i^\alpha(r,t)} \qquad (i = 1, 2, ..., p) \qquad (4a)$$

$$\frac{d\eta_i^\beta(r,t)}{dt} = -L_i^\beta \frac{\delta F}{\delta\eta_i^\beta(r,t)} \qquad (i = 1, 2, ..., q) \qquad (4b)$$

$$\frac{dC(r,t)}{dt} = \nabla\left\{ L_C \nabla\left[\frac{\delta F}{\delta C(r,t)} \right] \right\} \qquad (4c)$$

where L_i^α, L_i^β and L_C are kinetic coefficients related to grain boundary mobilities and atomic diffusion coefficients, t is time, and F is the total free energy given in Eq. (2).

III. Numerical Methodology

To numerically solve the set of kinetic equations (4), one needs to discretize them with respect to space. We discretize the Laplacian using the following approximation:

$$\nabla^2\phi = \frac{1}{(\Delta x)^2}\left[\frac{1}{2}\sum_j(\phi_j - \phi_i) + \frac{1}{4}\sum_{j'}(\phi_{j'} - \phi_i) \right] \qquad (5)$$

where ϕ is any function, Δx is the grid size, j represents the set of first nearest neighbors of i, and j' is the set of second nearest neighbors of i. For discretization with respect to time, we employed the following simple Euler technique,

$$\phi(t+\Delta t) = \phi(t) + \frac{d\phi}{dt} \times \Delta t \qquad (6)$$

where Δt is the time step for integration which is chosen small enough to avoid numerical instability. All of the results discussed below were obtained by using $\Delta x = 2.0$, $\Delta t = 0.1$ to ensure the numerical stability. The kinetic equations are discretized using 512 × 512 points with periodic boundary conditions applied along both directions. The total number of orientation field variables for two phases are 30.

In the Al_2O_3–ZrO_2 systems, it was reported[22,23] that the average ratio of the grain boundary energy to the interphase energy for the Al_2O_3 phase (denoted as α phase) is $R_\alpha = \sigma_{alu}^\alpha/\sigma_{int}^{\alpha\beta} = 1.4$, and that for the ZrO_2 phase (denoted as β phase) is $R_\beta = \sigma_{zir}^\beta/\sigma_{int}^{\alpha\beta} = 0.97$. We assume that both grain boundary and interphase boundary energies are isotropic. It is found that parameters $A = 2.0$, $B = 9.88$, $C_\alpha = 0.01$, $C_\beta = 0.99$, $D_\alpha = D_\beta = 1.52$, $\gamma_\alpha = \gamma_\beta = 1.23$, $\delta_\alpha = \delta_\beta = 1.0$, $\varepsilon = 7.0$, $\kappa_C = 1.5$, $\kappa_i^\alpha = 2.5$, and $\kappa_i^\alpha = 2.0$, give the correct grain boundary to interphase boundary ratios for the Al_2O_3–ZrO_2 system.[14]

All of the kinetic data and size distributions were obtained using 512 × 512 grid points and averaged from several independent runs. There are more than 2700 grains at the beginning of collecting data for calculating the statistics and there are about 200 at the end. To generate the initial two-phase microstructure, a single-phase grain growth simulation was first performed to obtain a fine grain structure. Grains are then randomly assigned with the equilibrium composition C_α or C_β and an orientation field, keeping the overall average composition corresponding to the desired equilibrium volume fractions.

IV. Simulation Results and Discussion

(1) Effect of Volume Fraction on Coarsening Rate

The details of two-phase microstructures and their evolution in ZrO_2–Al_2O_3 two-phase solids have been previously dis-

cussed.[14] Six representative simulated two-phase microstructures at six different volume fractions of the ZrO_2 phase are shown in Fig. 2. The temporal microstructural evolution in a system with 50% ZrO_2 phase is shown in Fig. 3. In these microstructures, ZrO_2 grains are bright and Al_2O_3 grains are gray. The time dependencies of the average grain size in the 50% ZrO_2 system with the initial microstructure generated from a fine grain structure are shown in Fig. 4 for Al_2O_3 (α phase). In this plot, the solid line is a nonlinear fit to the power growth law $R_t^m - R_0^m = kt$. According to Fig. 4, the coarsening kinetics for the α phase follows the power law with $m = 3$ and $k = 4.31$. Since $R_\alpha \neq R_\beta$, it is expected that the coarsening kinetics of α and β phase grains will be different. Indeed, it is found that, in the β phase, the average grain size increases with time with a power law with $m = 3$ and $k = 3.8$, which indicates that the α phase (Al_2O_3) has a larger coarsening kinetic coefficient k because of its higher grain boundary energy. In a binary system, the kinetic coefficient k is proportional to the diffusivity and interfacial energies.[18] Therefore, the higher the interfacial energies, the larger the kinetic coefficient. Our simulation results agree with those theoretical predictions.

To illustrate the effect of the volume fraction on the coarsening kinetics of two-phase solids, the coarsening kinetics in systems with 10% and 50% ZrO_2 (β) phase are compared in Fig. 5, in which R^3 is plotted against t. The kinetic coefficient k for the 90% Al_2O_3 (α) phase is 31.85, and that for the 10% β phase is 0.785. Hence, the volume fraction has a dramatic effect on the coarsening kinetics for both phases. The kinetic coefficient k for the 90% α phase is about an order of magnitude larger than that for the 50% α phase ($k = 4.31$) while the

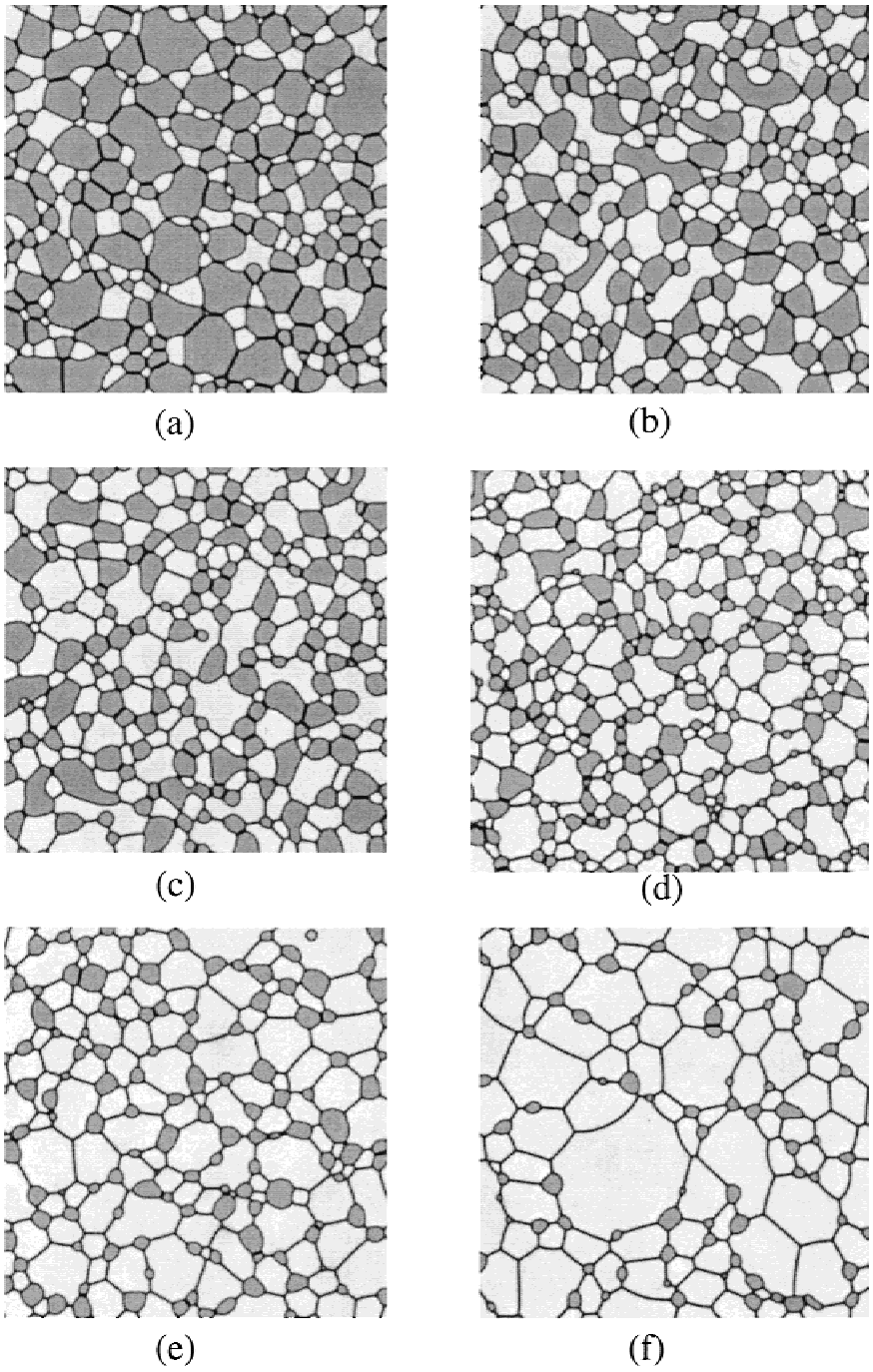

Fig. 2. Typical microstructures in Al_2O_3–ZrO_2 systems with different volume fractions of ZrO_2 phase: (a) 30%, (b) 50%, (c) 60%, (d) 70%, (e) 80%, (f) 90%. System size is 512 × 512.

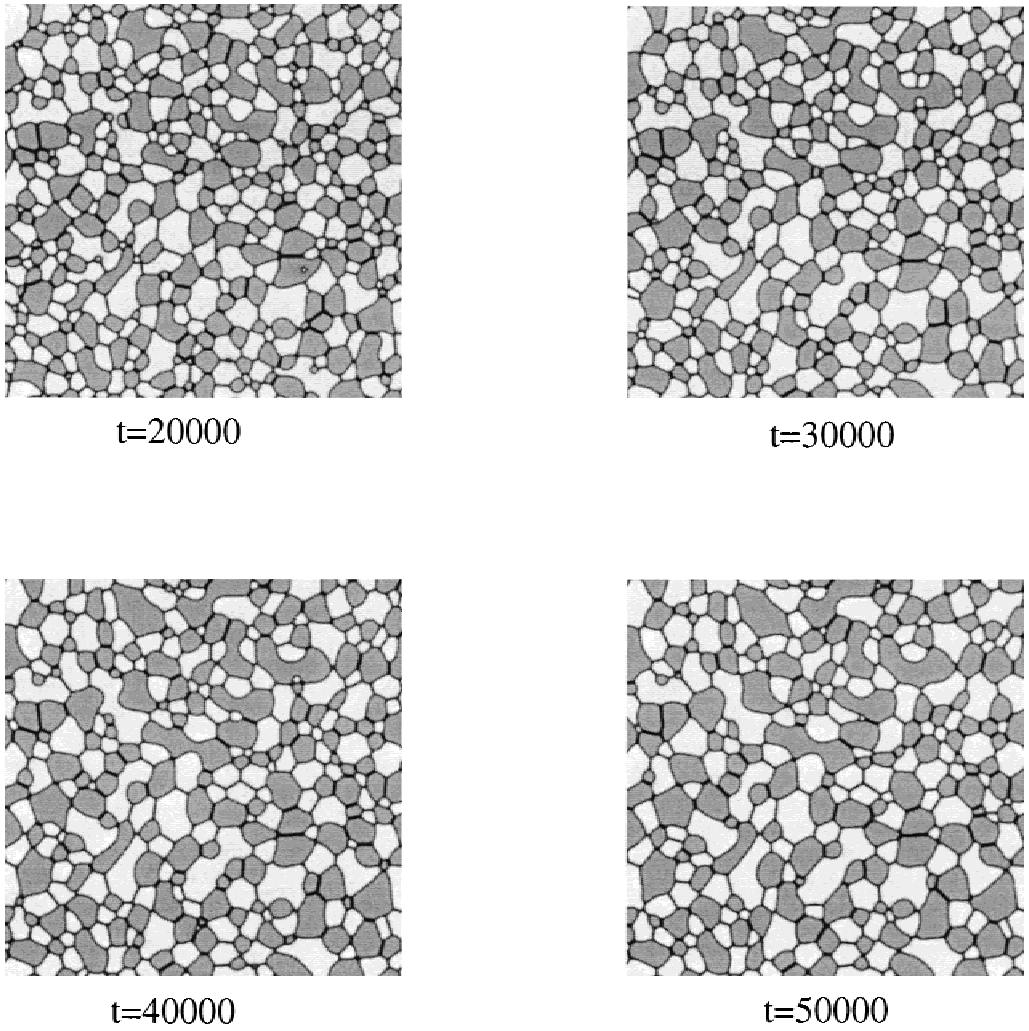

Fig. 3. Microstructural evolution in the Al_2O_3–50% ZrO_2 system. $R_\alpha = 1.4$, $R_\beta = 0.97$. System size is 512 × 512.

k value for the 10% β phase is 5 times smaller than the 50% β phase. As a result, the difference in *k* values for α and β phases is about 50 times. This dramatic change comes from the different diffusion distances involved for coarsening as the volume fraction changes. For systems with low volume fraction β, the coarsening kinetics of β phase grains is solely controlled by Ostwald ripening and the typical diffusion distance is about the typical separation distance between β phase grains; the coarsening kinetics of the α phase depends on the fraction of its grain boundaries that are pinned by β grains, and therefore the volume fraction of β.

The dependence of the growth exponent *m* on the volume fraction of ZrO_2 (β phase), extracted from the nonlinear fits to the kinetic data, is summarized in Fig. 6. It is obvious that, for both phases, the growth exponent $m = 3$ is independent of the volume fraction of the second phase, indicating that the coarsening is always controlled by the long-range diffusion process in two-phase solids. The predicted kinetic coefficients at different volume fractions are compared with experimental results in Al_2O_3–cubic ZrO_2 (YZTA) in Fig. 7, and in the Ce-doped Al_2O_3–ZrO_2 (CeZTA) system in Fig. 8. In Fig. 7, all kinetic coefficients were normalized with the experimental values for YZTA at 50% ZrO_2 by Harmer *et al.*,[24] while in Fig. 8 they were normalized with the experimental values for CeZTA at 40% ZrO_2 from Alexander *et al.*[25] It can be seen that the trend of the kinetic coefficient variation with volume fraction predicted by simulations agrees very well with experimental results in both systems, even though the differences of diffusivities and mobilities between two phases are not distinguished in

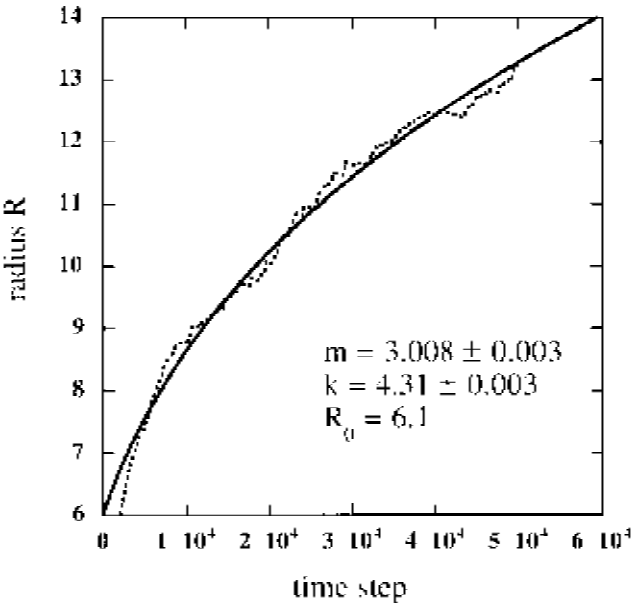

Fig. 4. Time dependence of the average grain size of Al_2O_3 phase. The volume fraction of ZrO_2 phase is 50%. $R_\alpha = 1.4$, $R_\beta = 0.97$. The dots are the measured data from simulated microstructures. The solid line is a nonlinear fit to the power-growth law $R_t^m - R_0^m = kt$ with three variables *m*, *k*, and R_0.

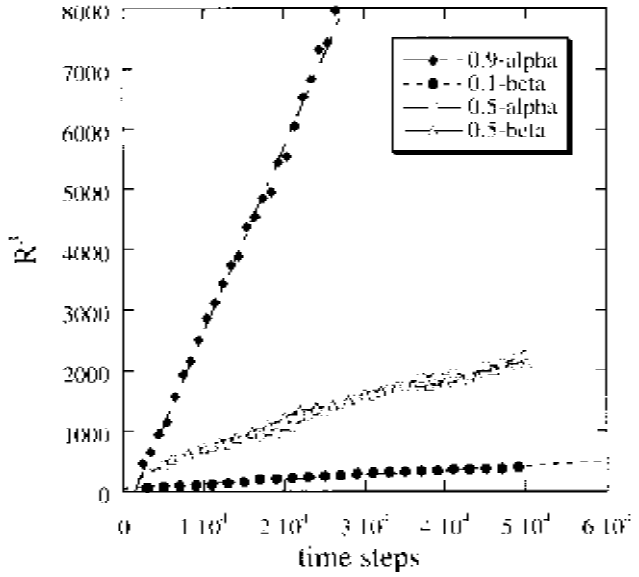

Fig. 5. Effect of volume fractions on the coarsening kinetics in the Al_2O_3–ZrO_2 system. The volume fractions of ZrO_2 phase are 10% and 50%. $R_\alpha = 1.4$, $R_\beta = 0.97$.

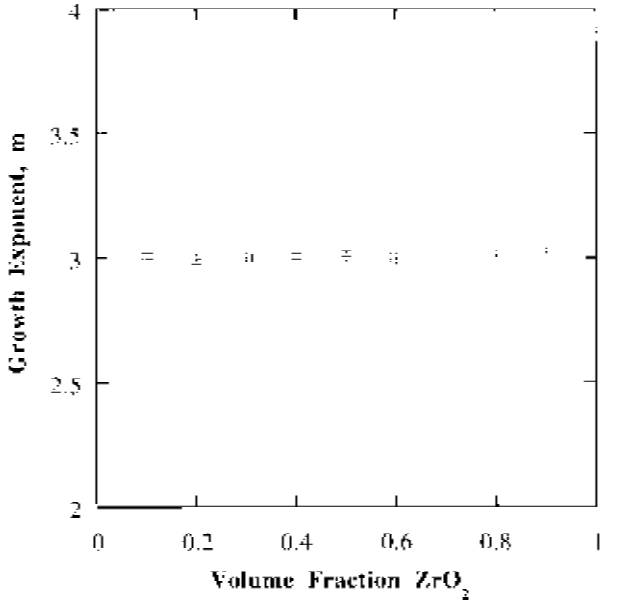

Fig. 6. Effect of volume fractions on growth exponent m in Al_2O_3–ZrO_2 systems $R_\alpha = 1.4$, $R_\beta = 0.97$.

the current simulations. Both simulations and experimental results showed that kinetic coefficients have a minimum value at 50% volume fraction, indicating the slowest grain growth kinetics at this volume fraction for Al_2O_3–ZrO_2 composites. This can be easily understood from the 50% microstructures, in which most grain boundaries of two phases are pinned by the other phase grains and the movement of grain boundaries is significantly retarded. It should be pointed out that although we can hardly make any quantitative comparisons for the kinetic coefficients between our 2-D simulations and experimental measurements on 3-D systems, it is interesting that very similar trends for the variation of the kinetic coefficient with the volume fraction were obtained in simulations and experiments.

(2) Effect of Volume Fraction on Grain Size Distributions

The time dependence of grain size distributions in the 50% ZrO_2 system is shown in Fig. 9 for ZrO_2 (β phase). It can be

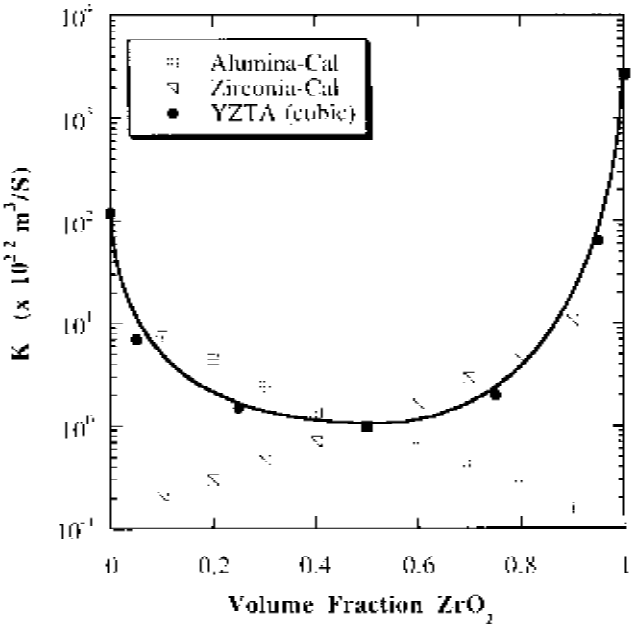

Fig. 7. Effect of volume fractions on kinetic coefficient k in Al_2O_3–ZrO_2 systems. Comparison of simulation results with experimental results for YZTA composite. (Adapted from M. P. Harmer *et al.*[24]) $R_\alpha = 1.4$, $R_\beta = 0.97$.

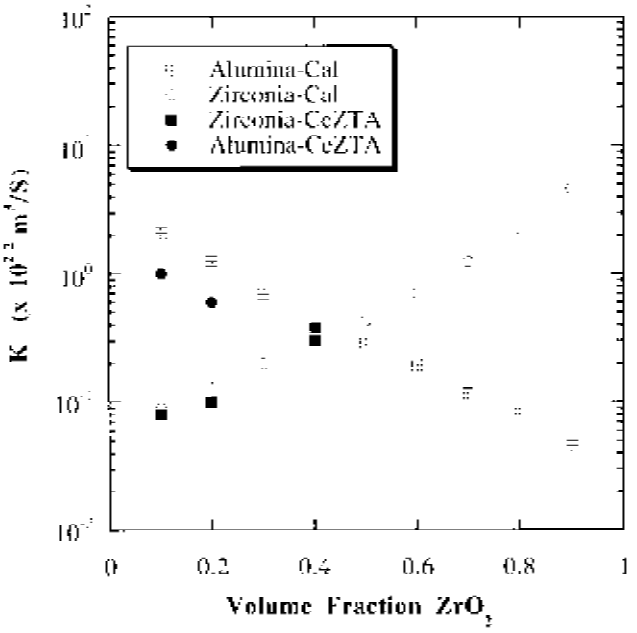

Fig. 8. Effect of volume fractions on kinetic coefficient k in Al_2O_3–ZrO_2 systems. Comparison of simulation results with experimental results for CeZTA composite. (Adapted from K. B. Alexander.[25]) $R_\alpha = 1.4$, $R_\beta = 0.97$.

seen that these distributions are self-similar and time-invariant, indicating the system has reached the steady state. Figure 10 shows the size distributions of the ZrO_2 phase at different time steps in the 10% ZrO_2 system. Scaling of size distributions is also observed. However, the shapes of these distributions are more peaked than those in the 50% system. The effects of volume fractions on size distributions of the second phase (ZrO_2) and matrix phase (Al_2O_3 in this case) are shown in Figs. 11 and 12, respectively. It can be seen that the size distributions of the ZrO_2 phase become broader as the volume fraction of

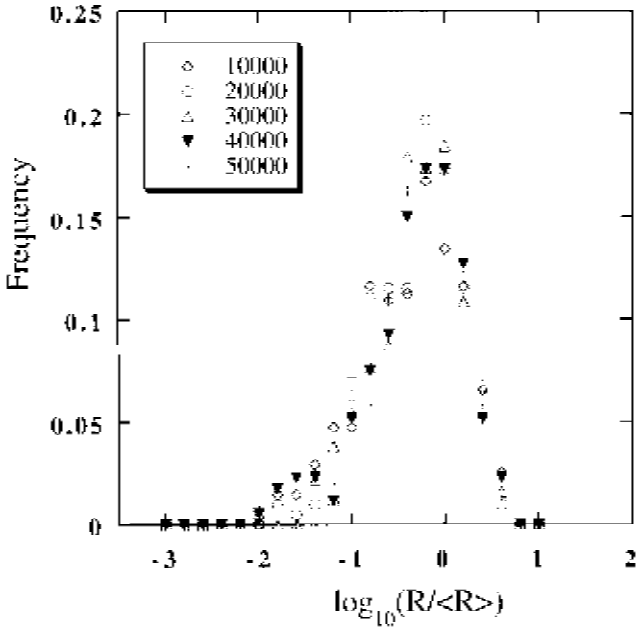

Fig 9. Time dependence of grain size distributions of ZrO_2 phases. The volume fractions of ZrO_2 phase are 50%. $R_\alpha = 1.4$, $R_\beta = 0.97$. Time step = 10 000, 20 000, 30 000, 40 000, 50 000. There are about 300 ZrO_2 phase grains at the 10 000 time step and 150 ZrO_2 phase grains at the 50 000 time step.

ZrO_2 phase increases from 10% to 50% while the size distributions of the matrix phase (Al_2O_3) are not significantly affected (Fig. 12). In the low volume fraction regime, second-phase particles are distributed at grain boundaries and corners of the matrix phase, which results in a narrow and peaked distribution. As the volume fraction of the second phase increases, grains of two phases become interconnected, which leads to a wider distribution. These characteristics can be

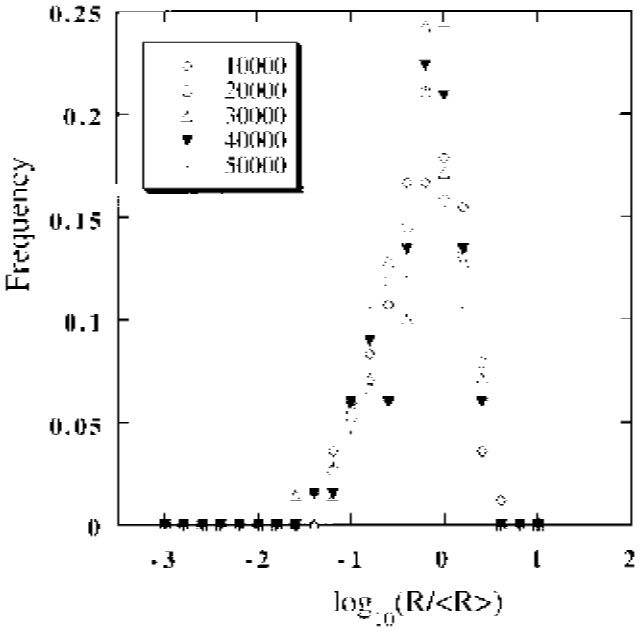

Fig 10. Time dependence of grain size distributions of ZrO_2 phases. The volume fractions of ZrO_2 phase are 10%. $R_\alpha = 1.4$, $R_\beta = 0.97$. Time step = 10 000, 20 000, 30 000, 40 000, 50 000. There are about 100 ZrO_2 phase grains at the 10 000 time step and 70 ZrO_2 phase grains at the 50 000 time step.

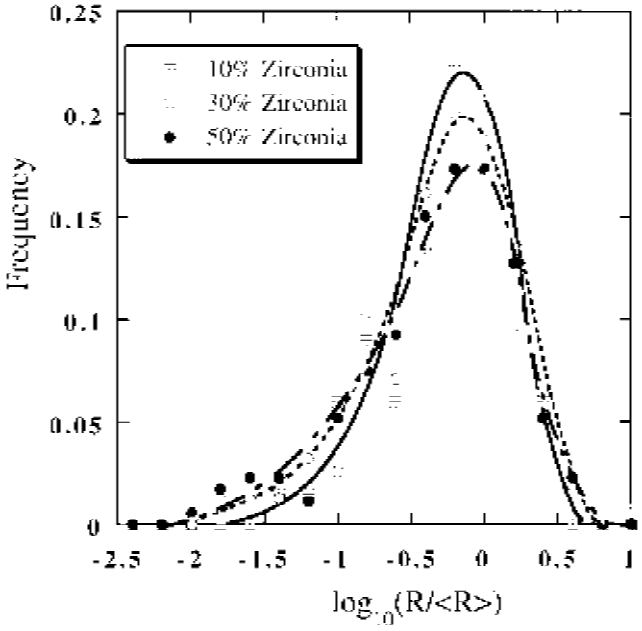

Fig 11. Effect of volume fractions on the grain size distributions of ZrO_2 phases $R_\alpha = 1.4$, $R_\beta = 0.97$.

clearly seen in simulated microstructures (Fig. 2). Therefore, these results suggest that there may not be a unique size distribution in steady state for two-phase systems; the size distributions are dependent on the volume fractions of the two phases.

(3) Effect of the Initial Microstructures

All the above results for Al_2O_3–ZrO_2 systems were obtained from initial microstructures generated from a fine single-phase grain structure. To study the effect of initial microstructures on the kinetics and size distributions of a two-phase system, we use a different method to generate the initial microstructures, i.e., direct crystallization of both solid phases from a liquid. Figure 13 is a comparison of the coarsening kinetics in the 50%

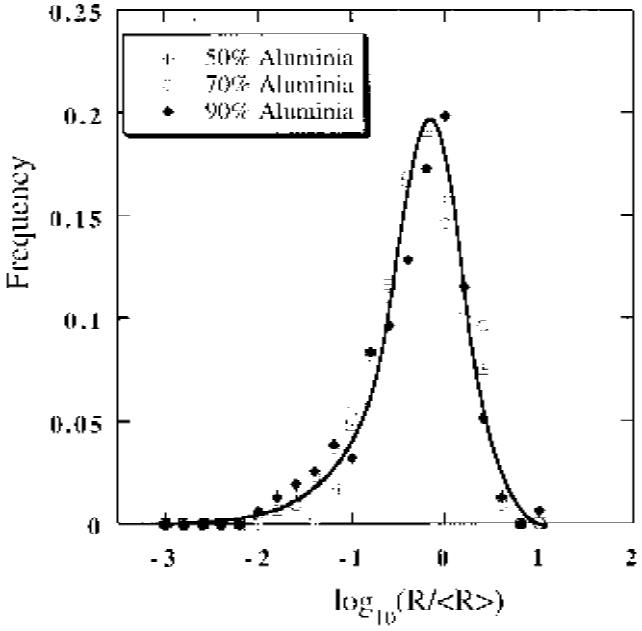

Fig 12. Effect of volume fractions on the grain size distributions of Al_2O_3 phases $R_\alpha = 1.4$, $R_\beta = 0.97$.

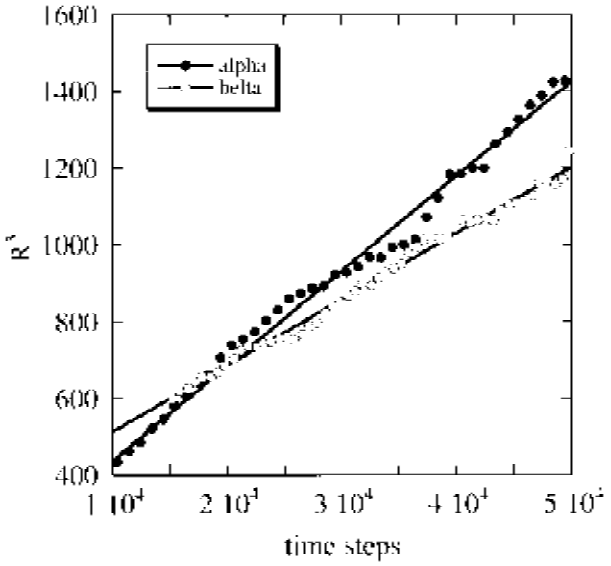

Fig. 13. Comparison of coarsening kinetics of the Al_2O_3 (α) and ZrO_2 (β) phases in the system with 50% ZrO_2. The initial structure is generated from a liquid.

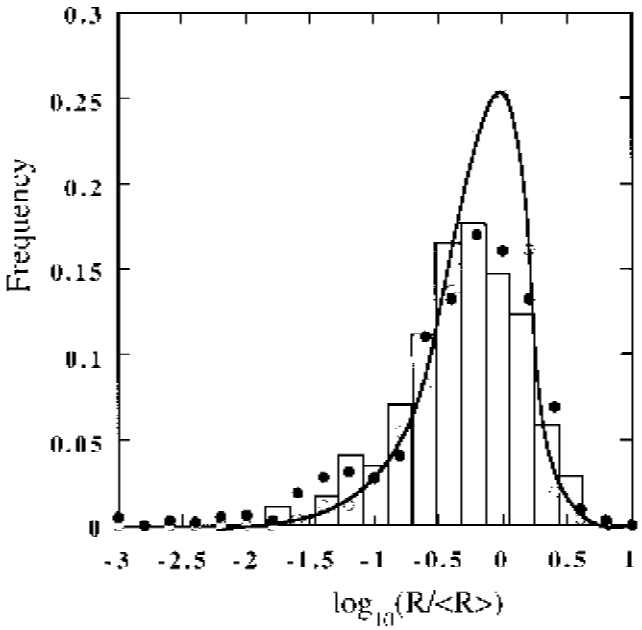

Fig. 14. Effect of the initial microstructure on the steady-state grain size distributions of Al_2O_3 phase in the system with 50% ZrO_2. The open dots represent the size distribution of Al_2O_3 with the initial structure generated from a liquid (the solid line is a guide to the eyes); the histogram is the size distribution of Al_2O_3 with the initial structure created from a fine grain structure; the solid dots represent the size distribution of the initial fine grain structure.

ZrO_2 system for the α and β phases with the initial microstructure generated from a liquid. To clarify the difference, R^3 is plotted against time steps. Under this initial condition, the average grain size increases with time following the power law with $m = 3$ and the coefficient k is 2.51 for the α phase and is 1.99 for the β phase, respectively. Comparing with the results obtained from the initial microstructures generated from a fine grain structure (Figs. 3 and 4), it is clear that the grain growth exponent m is independent of the initial microstructures, whereas the kinetic coefficients k are about 2 times smaller than those obtained with the initial microstructure generated from a fine grain structure, in which $m = 3$, $k = 4.31$ for the α phase and $k = 3.8$ for the β phase. The reason for the retardation of grain growth kinetics is that, when the initial two-phase structure is generated from the solidification of an initial unstable liquid, grains of the α and β phase are alternately distributed, i.e., each α grain having β grains as nearest neighbors and vice versa. When the initial microstructure is generated from a fine grain structure, there exist clusters of the same phase grains. Within the clusters of the same phase grains, grain growth occurs faster, which results in larger kinetic coefficients. It should be pointed out that the differences in the kinetic coefficients k resulting from different initial microstructures are small, comparing with the influence of volume fractions on the kinetics.

The effect of the initial microstructures on the grain size distributions is compared in Fig. 14. In this plot, the open dots represent a typical size distribution with the initial microstructure generated from a liquid (the solid line is just a guide to human eyes), the histogram is the size distribution with the initial structure created from a fine grain structure with the solid dots representing the size distribution of this initial fine grain structure. It can be seen that size distributions from different initial microstructures are quite different. The size distribution of the initial structure generated from a liquid is much sharper than that obtained from the initial microstructure generated from a fine grain structure. On the other hand, the size distribution with the initial microstructure generated from a fine grain structure is almost identical to the original distribution of that fine grain structure. Therefore, in two-phase systems, size distributions are also dependent on the initial microstructures and there are no unique size distributions for a given volume fraction and given ratios of grain boundary energies to the interphase boundary energy.

(4) Relationship between Matrix Grain Size and Second-Phase Particle Size

From a microstructural control point of view, there is an important relationship between the matrix grain size and the size and volume fraction of the second-phase particles. From the original work of Smith and Zener,[26] it is predicted that D/r should be proportional to $1/f$, where D is the average grain size of the matrix phase when the grain growth stops, r is the radius of second-phase particles, and f is the volume fraction of the second phase. Recently, Hellman and Hillert[27] showed that the D/r is proportional to $1/f^{1/3}$ for high volume fractions and a nonrandom distribution of the second-phase particles. On the other hand, using Monte Carlo simulations, Srolovitz *et al.*[10] showed that the D/r is proportional to $1/f^{1/2}$ in 2-D, and the same relationship was also obtained by Doherty *et al.*[28] for 3-D systems by assuming all particles distributed at grain boundaries.

We examine the relationship between matrix grain size and second-phase particle size by plotting the matrix grain size D vs. $r/f^{1/2}$ in Al_2O_3-rich two-phase systems from our 2-D computer simulations (Fig. 15). It is found that the relation $D = Ar/f^{1/2}$ is followed reasonably well for volume fractions less than 30%, with the constant A values being 1.32 for Al_2O_3-rich systems and 1.27 for ZrO_2-rich systems. These A values are much smaller than 3.4, which was obtained by Srolovitz *et al.*[10] for small and immobile particles. The smaller A values mean a smaller matrix grain size at a certain size of second-phase particles. Therefore, the pinning effect of second-phase grains is stronger than it is in systems with small and noncoarsening particles. One reason responsible for the large pinning effect in Al_2O_3–ZrO_2 two-phase solid is that the sizes of second-phase particles are large and it is almost impossible for grain boundaries to pass through these particles. When the volume fraction of the second phase is larger than 40%, the relation $D = Ar/f^{1/2}$ is not followed anymore, which may result from the fact that at this volume fraction the second-phase grains become interconnected in a two-phase microstructure. However, experimentally, it was shown that the relation $D = Ar/f^{1/3}$ is followed for

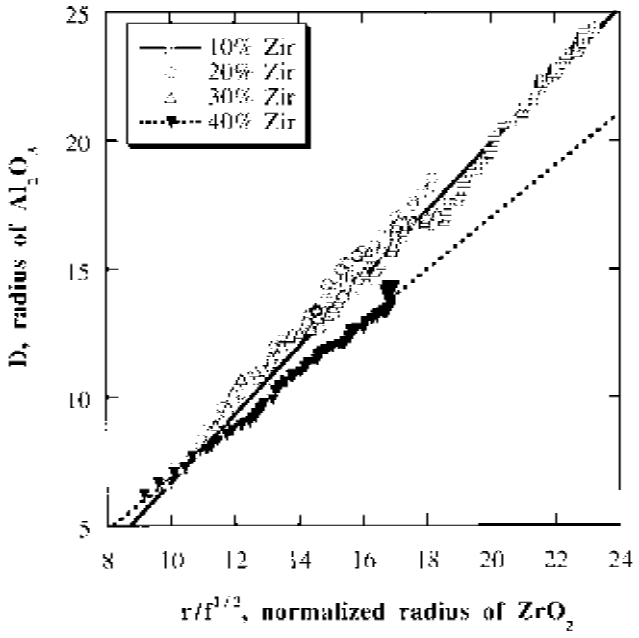

Fig. 15. Relations of the matrix grain size D with the second-phase particle size r normalized with $1/f^{1/2}$ for Al_2O_3–ZrO_2 two-phase systems. The Al_2O_3 phase is the matrix phase.

volume fractions of the second phase less than 10% in 3-D Al_2O_3–ZrO_2 two-phase solids.[22] Therefore, it seems that the relationships between matrix grain size and second-phase particle size in 2-D and in 3-D systems can be very different.

V. Conclusions

The kinetics of the coupled grain growth in the Al_2O_3–ZrO_2 two-phase composites have been studied through computer simulations. The simulation results show that the kinetics and microstructural evolutions are in excellent qualitative agreement with experimental observations for Al_2O_3–ZrO_2 two-phase composites. It is found that the coupled grain growth and Ostwald ripening in volume-conserved two-phase systems is controlled by long-range diffusion and follows the power-growth law $R_t^m - R_0^m = kt$ with $m = 3$, which is independent of initial microstructures and the volume fraction of the second phase. However, the kinetic coefficient k depends on the grain boundary energies, the interphase boundary energy, initial microstructures, and volume fractions; among these factors, volume fraction of two phases has the most significant effect. The dependence of kinetic coefficient on volume fraction, predicted by the computer simulations, agrees very well with experimental measurements, at least qualitatively. Scaling of grain size distributions is observed in all circumstances, i.e., they are time-invariant in the steady state. However, the characteristics of size distributions vary with the initial microstructures and volume fractions. It is found that the relationship between matrix grain size and second-phase grain size follows $D = Ar/f^{1/2}$ in the 2-D simulations when the volume fraction of the second phase is less than 30%, which is different from the experimentally determined relationship, $D = Ar/f^{1/3}$ in 3-D.

Acknowledgment: We are grateful to Dr. K. B. Alexander for providing us a copy of her short-course notes given at the 1995 ACerS Annual Meeting.

References

[1]J. D. French, M. P. Harmer, H. M. Chan, and G. A. Miller, ''Coarsening-Resistant Dual-Phase Interpenetrating Microstructures,'' *J. Am. Ceram. Soc.*, **73,** 2508 (1990).

[2]F. F. Lange and M. M. Hirlinger, ''Grain Growth in Two-Phase Ceramics: Al_2O_3 Inclusions in ZrO_2,'' *J. Am. Ceram. Soc.*, **70,** 827 (1987).

[3]K. B. Alexander, P. F. Becher, S. B. Waters, and A. Bleier, ''Grain Growth Kinetics in Alumina–Zirconia (CeZTA) Composites,'' *J. Am. Ceram. Soc.*, **77,** 939 (1994), and references therein.

[4]B. Kibbel and A. H. Heuer, ''Exaggerated Grain Growth in ZrO_2-Toughened Al_2O_3,'' *J. Am. Ceram. Soc.*, **69,** 231 (1986).

[5]J. Wang and R. Raj, ''Activation Energy for the Sintering of Two-Phase Alumina/Zirconia Ceramics,'' *J. Am. Ceram. Soc.*, **74,** 1959 (1991).

[6]S. R. Witek and E. P. Butler, ''Zirconia Particle Coarsening and the Effects of Zirconia Additions on the Mechanical Properties of Certain Commercial Aluminas,'' *J. Am. Ceram. Soc.*, **69,** 523 (1986).

[7]C. S. Smith, ''Grains, Phases, and Interfaces: An Interpretation of Microstructure,'' *Trans. AIME*, **175,** 15 (1948).

[8]M. Hillert, ''Inhibition of Grain Growth by Second-Phase Particles,'' *Acta Metall.*, **36,** 3177 (1988).

[9]G. Grewal and S. Ankem, ''Modeling Matrix Grain Growth in the Presence of Growing Second Phase Particles in Two Phase Alloys,'' *Acta Metall. Mater.*, **38,** 1607 (1990).

[10]D. J. Srolovitz, M. P. Anderson, G. S. Grest, and P. S. Sahni, ''Computer Simulation of Grain Growth—III. Influence of a Particle Dispersion,'' *Acta Metall.*, **32,** 1429 (1984).

[11]G. N. Hassold, E. A. Holm, and D. J. Srolovitz, ''Effects of Particle Size on Inhibited Grain Growth,'' *Scr. Metall.*, **24,** 101 (1990).

[12]J. W. Cahn, ''Stability, Microstructural Evolution, Grain Growth, and Coarsening in a Two-Dimensional Two-Phase Microstructure,'' *Acta Metall. Mater.*, **39,** 2189 (1991).

[13]E. A. Holm, D. J. Srolovitz, and J. W. Cahn, ''Microstructural Evolution in Two-Dimensional Two-Phase Polycrystals,'' *Acta Metall. Mater.*, **41,** 1119 (1993).

[14]L.-Q. Chen and D. Fan, ''Computer Simulation Model for Coupled Grain Growth and Ostwald Ripening—Application to Al_2O_3–ZrO_2 Two-Phase Systems,'' *J. Am. Ceram. Soc.*, **79,** 1163 (1996).

[15]D. Fan and L.-Q. Chen, ''Diffusion-Controlled Grain Growth in Two-Phase Solids,'' *Acta Mater.*, in press.

[16]H. V. Atkinson, ''Theory of Normal Grain Growth in Pure Single Phase Systems,'' *Acta Metall.*, **36,** 469 (1988).

[17]J. A. Glazier and D. Weaire, ''The Kinetics of Cellular Patterns,'' *J. Phys.: Condens. Matter*, **4,** 1867 (1992).

[18]P. W. Voorhees, ''Ostwald Ripening of Two-Phase Mixtures,'' *Annu. Rev. Mater. Sci.*, **22,** 197 (1992), and references therein.

[19]D. Fan and L.-Q. Chen, ''Topological Evolution During Coupled Grain Growth and Ostwald Ripening in Volume-Conserved 2-D Two-Phase Polycrystals,'' *Acta Mater.*

[20]S. M. Allen and J. W. Cahn, ''A Microscopic Theory for Antiphase Domain Boundary Motion and Its Application to Antiphase Domain Coarsening,'' *Acta Metall.*, **27,** 1085 (1979).

[21]J. W. Cahn, ''On Spinodal Decomposition,'' *Acta Metall.*, **9,** 795 (1961).

[22]I-W. Chen and L. A. Xue, ''Development of Superplastic Structural Ceramics,'' *J. Am. Ceram. Soc.*, **73,** 2585 (1990).

[23]G. Lee and I-W. Chen, ''Sintering and Grain Growth in Tetragonal and Cubic Zirconia''; pp. 340–46 in *Sintering '87*, Proceedings of the 4th International Symposium on Science and Technology of Sintering (Tokyo, Japan, 1987), Vol. 1. Edited by S. Somiya, M. Shimada, M. Yoshimura, and R. Watanabe. Elsevier Applied Science, London, U.K., 1988.

[24]M. P. Harmer, H. M. Chen, and G. A. Miller, ''Unique Opportunities for Microstructural Engineering with Duplex and Laminar Ceramic Composite,'' *J. Am. Ceram. Soc.*, **75,** 1715 (1992).

[25]K. B. Alexander, ''Grain Growth and Microstructural Evolution in Two-Phase Systems: Alumina/Zirconia Composites''; Short Course on ''Sintering of Ceramics'' at the American Ceramic Society Annual Meeting, Cincinnati, OH, April 1995.

[26]C. S. Smith, ''Grains, Phases, and Interfaces: An Interpretation of Microstructure,'' *Trans. AIME*, **175,** 15 (1948).

[27]P. Hellman and M. Hillert, ''On the Effect of Second-Phase Particles on Grain Growth,'' *Scand. J. Met.*, **4,** 211 (1975).

[28]R. D. Doherty, D. J. Srolovitz, A. D. Rollett, and M. P. Anderson, ''On the Volume Fraction Dependence of Particle Limited Grain Growth,'' *Scr. Metall.*, **21,** 675 (1987). □